Supplementary Information: Interplay of Pressure, Modulation, and Disorder in the Superconductivity of $AuAgTe_4$

Y. Amiel,[‡a] E. Greenberg, [b] M. Diamond,[c#] Y.S. Ponosov,[d] N.M. Belozerova,[e,f] S. Chariton,[g] D. Zhang,[g,h] E.V. Lukin,[f] Y. J. Ryu,[g] A. Palevski,[a] and G. Kh. Rozenberg[*a]

[a] *School of Physics and Astronomy, Tel Aviv University, 69978 Tel Aviv, Israel.*

[b] *Applied Physics Division, Soreq NRC, Yavne 81800, Israel.*

[c] *X-ray Science Division, Advanced Photon Source, Argonne National Laboratory, Lemont, IL 60439, USA*

[d] *M.N. Mikheev Institute of Metal Physics UB RAS, S. Kovalevskaya Str. 18, 620137,*

Ekaterinburg, Russia

[e] *Moscow Center for Advanced Studies, Kulakova Str. 20, Moscow 123592, Russia;*

[f] *Frank Laboratory of Neutron Physics, Joint Institute for Nuclear Research, Joliot-Curie Str. 6, Dubna 141980, Russia*

[g] *GSECARS, The University of Chicago, 9700 S. Cass Ave, Lemont, IL 60439, USA*

[h] *School of Ocean and Earth Science and Technology, University of Hawai'i at Manoa, Honolulu, HI 96822, USA*

[#] *Current address: Department of Physics, United States Coast Guard Academy, New London, CT, 06320, USA*

***** *Correspondence: G. Kh. Rozenberg (emtsm@tauex.tau.ac.il)*

I. EXPERIMENTAL DETAILS

Samples. The high-pressure electrical resistance measurements were performed with high-quality natural single crystal of silvanite, AuAgTe4, from the private collection of Prof. Ladislav Bohat´y and Petra Becker-Bohat´y, University of Cologne [1]. The XRD and Raman experiments were carried out using natural single crystals of sylvanite from the Kochbulak deposit, Kuraminsky range, Uzbekistan. Their composition and structure were confirmed using a Cameca SX100 electron probe microanalyzer and a Jeol JSM6390LV scanning electron microscope with an Inca Energy 450 X-Max80 EDS detector. The atomic composition matches well the ideal sylvanite stoichiometry: observed deviations are ∼1-2 at.%, which is within the measurement error of 3%.

Transport measurements. For our transport measurements, pressure was generated using TAU opposing plate diamond anvil cells (DACs) [2] with diamond anvil culets of 400 μm. A pre-indented rhenium gasket was drilled and then filled and covered with a powder mixture of NaCl and Al_2O_3 for electrical insulation. Apiece of single-crystal AuAgTe4 with an average size of ∼ 0.02×0.02×0.01 mm3 was placed onto the culets. A Pt foil with a thickness of 5-7 μm was cut into triangular probes connecting the sample and the copper leads, allowing electrical transport measurements at elevated pressures. 6 probes were placed in each DAC. A few ruby fragments for pressure determination2 were located in the region between the Pt electrode tips overlapping the sample. No pressure-transmitting medium was used, but pressure is effectively transmitted to the sample upon compression by way of the surrounding NaCl + Al_2O_3 insulation. The ruby spectra suggest a ∼ 10% pressure inhomogeneity.

Electrical transport measurements were performed using a physical property measurement system (PPMS Quantum Design, USA). Two slots of resistance measurements were performed (runs 1, 2) up to ~23, and 12 GPa, respectively. The sample was compressed, decompressed and recompressed in increments of ~ 2 − 3 GPa on average, and cooled down from ambient temperature down to 2 K. After each pressure increment a temperature cycle was performed. Superconducting transition temperature T_c was defined at the midpoint of the transition curve (where resistance drops to 50% of the normal state value). Calculating the peak of the dR/dT derivative gives practically the same result. The onset and zero-resistance temperatures are reported separately when discussing the transition width, $\Delta T_c = T_c^{onset} - T_c^{zero}$ (Fig. S1). Ruby-line variations across the transport sample correspond to an estimated pressure inhomogeneity of approximately 10%.

X-ray Diffraction.

Pieces of single-crystal of $AuAgTe_4$ with an average size of 0.02x0.02x0.01 mm^3 were loaded into BX90-type DAC [3] equipped with Boehler-Almax diamonds with 300 μm culet size, typically along with a small ruby chip (for quick pressure estimation) and a small piece of Au. Most of the runs included gas loading of neon, which also served as a pressure standard. One run employed He as the pressure medium, and one additional run had a $NaCl/Al_2O_3$ pressure medium. The experiments were performed at specialized high-pressure beamlines at the APS synchrotron (Argonne, IL, USA). Details of the wavelength, spot size, pressure medium, and the detector used for collecting each data set are given in Table S1. Within the sample chamber, typically a piece of Au was added for pressure determination. For each compression/decompression run a LaB_6 standard was used to calibrate the beam position, sample-detector distance, and detector tilts. In most runs, since the sample started out as a single crystal, data was collected during a continuous rotation of the diamond anvil cell (DAC), typically from -30 to +30 in omega. All collected frames were summed up and the data in the current study was treated as powder data. The software DIOPTAS was used to integrate the raw 2D images into a 1D diffraction pattern, and to determine pressure from either Ne and/or Au [4]. GSAS II was used to perform LeBail refinements to obtain the unit-cell parameters [5].

High-pressure powder XRD measurements with methanol-ethanol (4:1) PTM were carried out up to 32 GPa using an Xeuss 3.0 instrument, Xenocs, France. Radiation was generated by a GeniX3D source (Mo-Kα edge, λ = 0.71078 Å) and detected using an Eiger2 R 1M 2D detector, Dectris, Switzerland. Each pressure point was exposed for 2 hr at room temperature. The experiments utilized a Boehler-Almax plate-type diamond anvil cell with diamonds featuring 600 μm culets. The sample was loaded into a 250 μm diameter hole in a Re gasket, indented to approximately 80 μm thickness. Pressure was measured using the ruby fluorescence technique with a typical determination error not exceeding 0.1 GPa. XRD data were analyzed using FullProf software [6].

Table S1. Details of the beamline, wavelength, spot size, pressure medium, and the detector used for collecting each data set.

Run	Beamline	Detector	Pressure Medium	Spot-size	Wavelength	
2021-3	IDD	Pilatus 1M CdTe	Neon	3x4 μm^2	0.2952 Å	Compression to 3.7 GPa

	BMD			6x10 μm^2		Compression from 3.7 to 27 GPa
	IDD			3x4 μm^2		Decompression from 27 GPa
2023-1	IDD	Pilatus 1M CdTe	Neon	3x4 μm^2	0.2952 Å	Compression to 22.4 GPa
						Compression from 22.4 to 33.6 GPa
2025-2 A	BMD	Pilatus 1M CdTe	Helium	1.6x5.7 μm^2	0.2952 Å	Compression to 36 GPa + decompression
2025-2 B	BMC	Pilatus 1M	NaCl+Al_2O_3	10x10 μm^2	0.4306 Å	Compression to 32.5 GPa + decompression
2026-1	IDD	Eiger2 X 9M CdTe	NaCl+Al_2O_3	1x1 μm^2	0.3344 Å	Mapping following decompression

Raman Spectroscopy.

In the cases of He, Ne, or a mixture NaCl/Al_2O_3 pressure-transmitting medium (PTM) Raman spectra were collected alongside some of the diffraction runs. Spectra were collected using the GSECARS Raman system [7], typically using a 532 nm excitation (for some measurements an excitation of 660 or 473 nm was used). The typical exposure time for each spectrum was 60 sec with a typical power on the sample of 2-40 mW over a diameter of ~4.5 μm. The spectral resolution was better than 2 cm^{-1}.

In the case of methanol-ethanol (4:1) PTM the Raman spectra were excited by low-power laser radiation (up to 3mW) at wavelengths of 532 nm and 633 nm, and they were recorded by Renishaw RM1000 microscope spectrometer, providing a focal spot on the samples of 2–10μm diameter, depending on settings. Another set of measurements was made using neon as a pressure-transmitting medium. In this set spectra were excited at wavelengths of 473 nm and 660 nm, and they were recorded by Princeton Instruments Acton 2500 spectrometer. The spectral resolution was about 3 cm^{-1}.

Pressure was measured by the ruby luminescence method.

To study the behavior of the quasi-elastic continuum, the measured phonon spectra (after extracting of the background from ME pressure medium) were fitted with Lorentzians superimposed on a polynomial background increasing toward low frequencies. The Raman susceptibility $\chi''(\omega)$ was estimated by dividing the latter curve by the Bose factor $(n(\omega)+1)$. Such quantitative measurements were carried out under compression up to ~13 GPa and decompression from high pressures (~26 GPa) in the pressure range of 15.1 - 1.0 GPa. The Raman susceptibility $\chi''(\omega)$ of the continuum at different pressures is shown in Fig. S7 a,b. The inset shows an approximation of the spectrum measured at 8.2 GPa. Note that at other measurement sets the background from ME PTM was not measured and therefore only qualitative information on the behavior of the quasi-elastic continuum can be obtained.

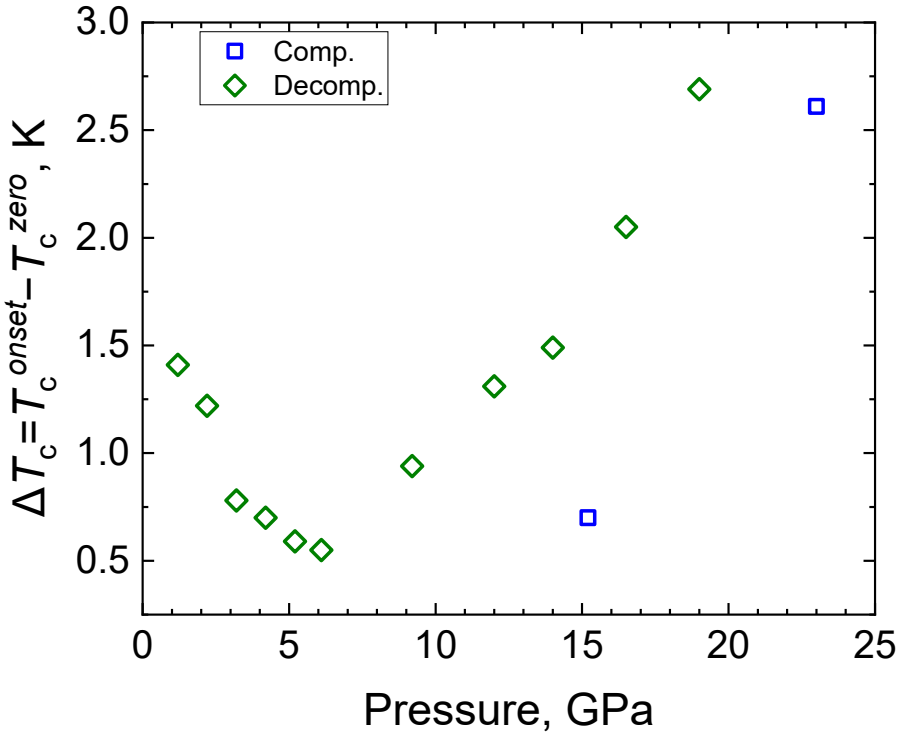

Fig. S1 Superconducting transition range versus pressure during compression and decompression (run 1).

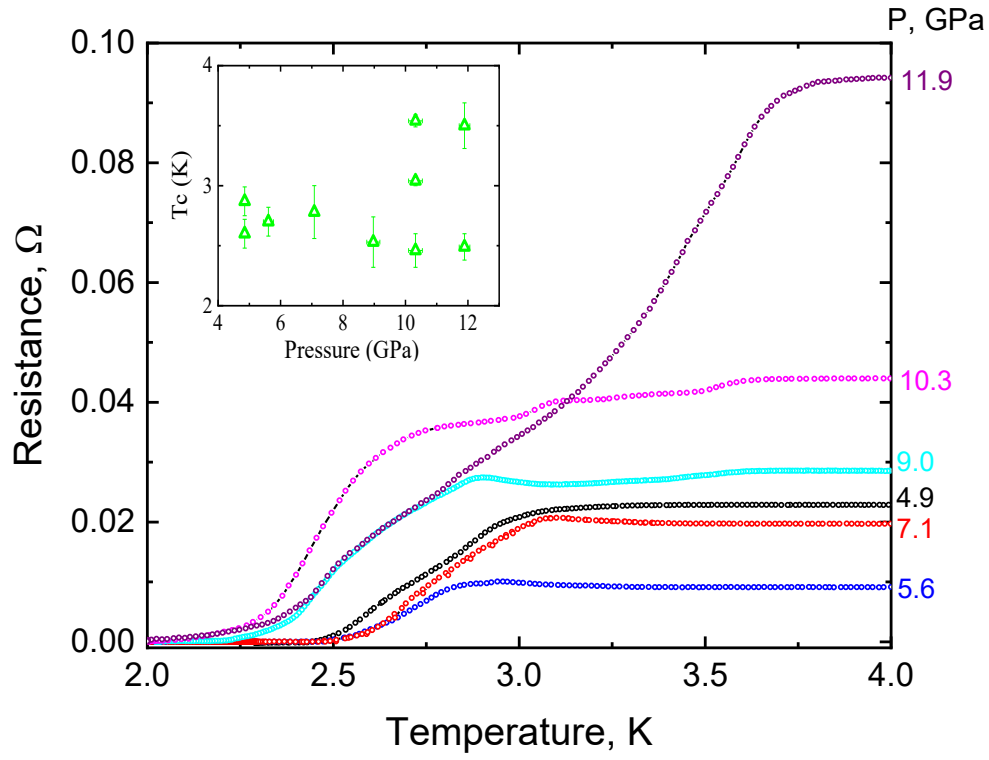

Fig. S2 Resistance versus temperature for $AuAgTe_4$ during compression (run 2). At ~10 GPa, a distinct second transition emerges with higher T_c ~ 3.5 K, becoming dominant by ~12 GPa. The inset: pressure dependence of T_c showing the appearance of the higher-T_c state above 10 GPa.

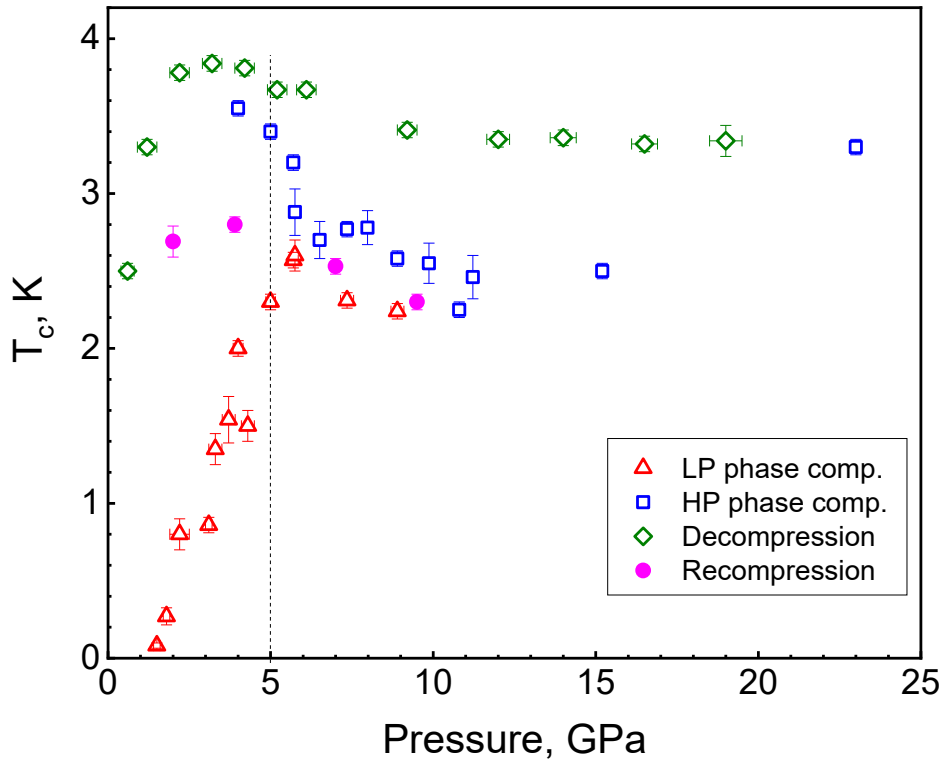

Fig. S3 Critical temperature as a function of pressure. Red symbols: compression through LP phase; blue symbols: compression through HP phase; green symbols: decompression; magenta symbols: recompression.

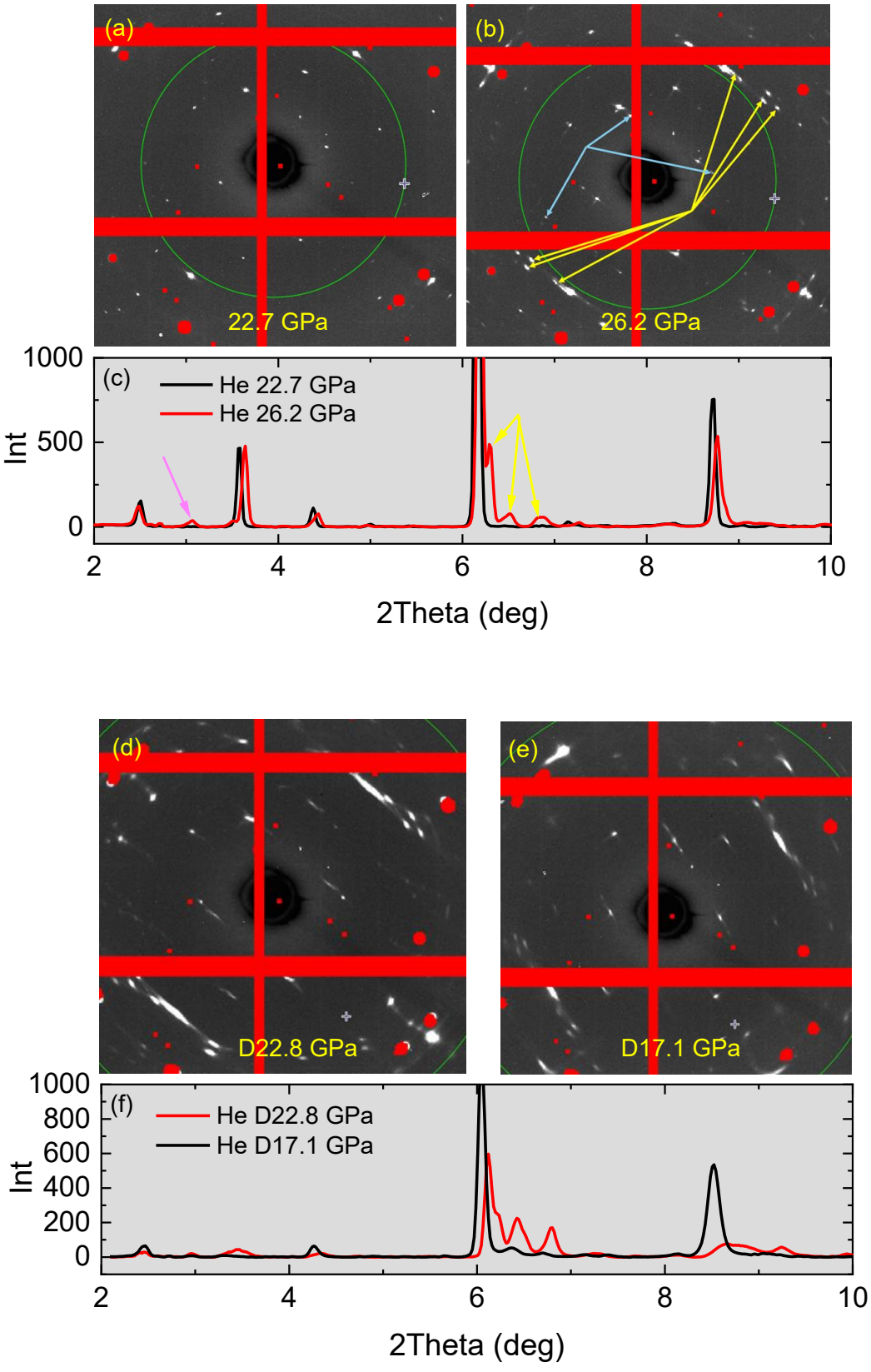

Fig. S4 Two-dimensional X-ray diffraction images and integrated patterns of $AuAgTe_4$ with helium pressure medium. (a, b) Compression: at 22.7 GPa the P2/m phase produces sharp diffraction spots; at 26.2 GPa these evolve into streaks with multiple intensity maxima (arrows). The streak pattern, rather than discrete spots, is the signature of incommensurate modulation. Panel (c) shows the integrated patterns, with the apparent diffraction lines caused by the

streak pattern. (d, e) Decompression: at D22.8 GPa and D17.1 GPa, weak streak features remain visible, consistent with the persistent but weakened modulation, as evidenced in (f).

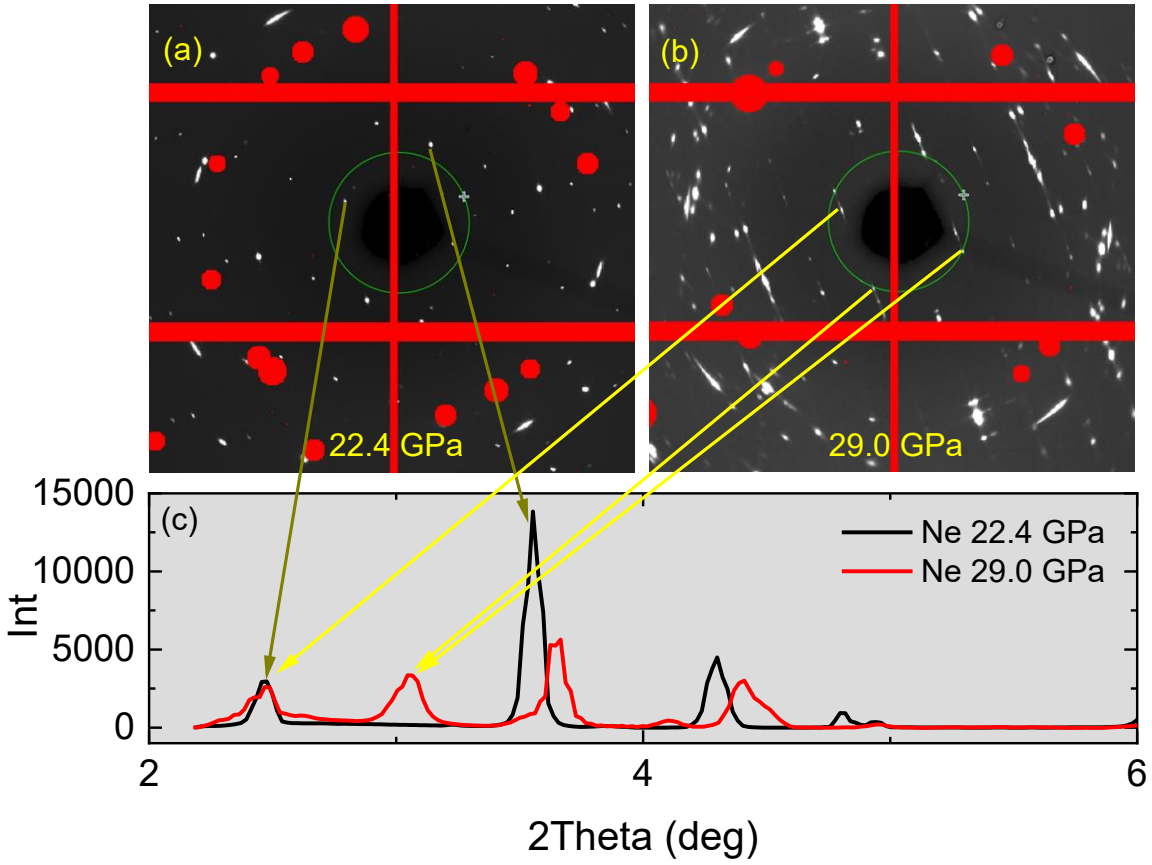

Fig. S5 Two-dimensional X-ray diffraction images and integrated patterns of $AuAgTe_4$ with neon pressure medium upon compression. At 29 GPa (b), in contrast to 22.4 GPa (a), the diffraction features form streaks with three intensity maxima (hot spots) along each streak, the signature of incommensurate modulation. Panel (c) shows the integrated patterns with the apparent diffraction lines due to the streak patterns.

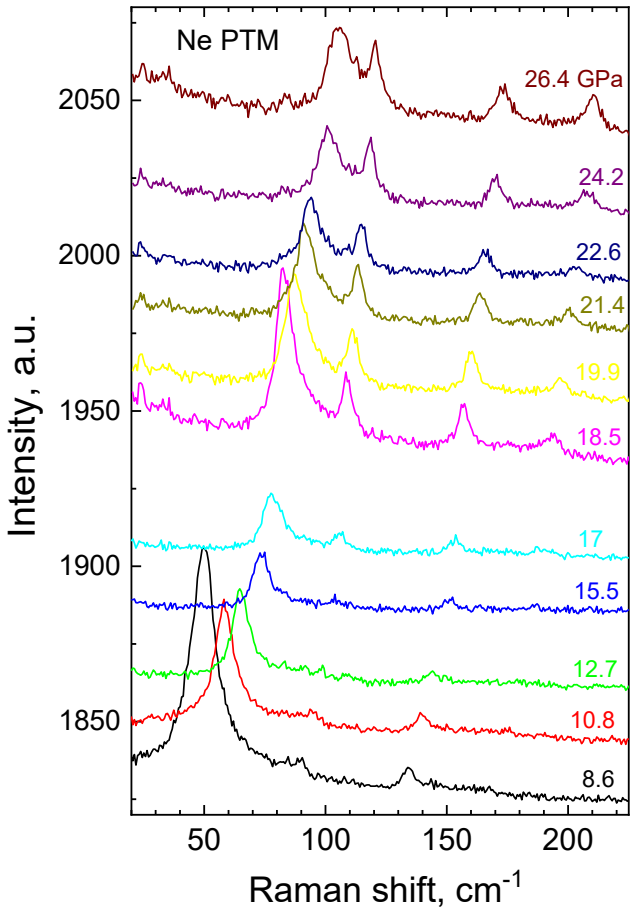

Fig. S6 Raman spectra of $AuAgTe_4$ upon compression from 8.6 to 26.4 GPa with neon pressure medium, showing HP phase modes evolving with pressure. The HP1 transition (observed at ~29 GPa in XRD; Fig. 3) was not reached in these Raman measurements.

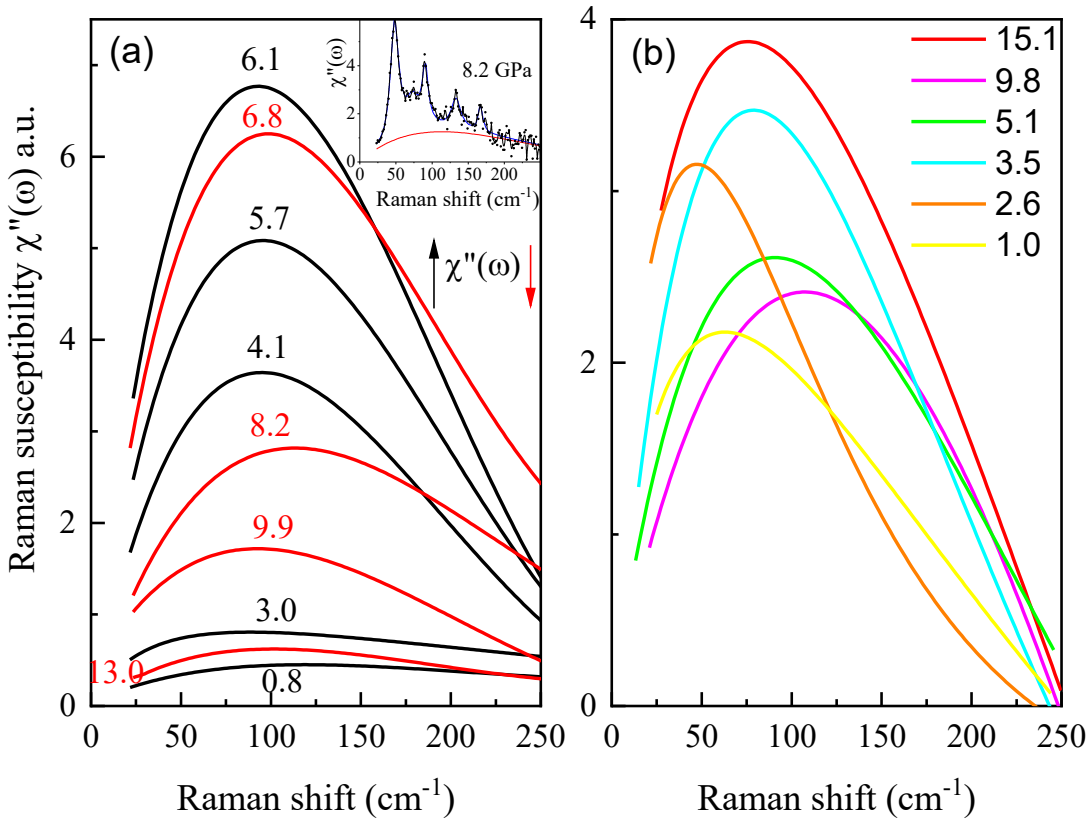

Fig. S7 The Raman susceptibility χ"(ω) of the continuum at different pressures upon compression (a) and decompression (b) from high pressures (~26 GPa). Note that upon compression the scattering intensity increases sharply at the LP-HP transition range and then decreases abruptly after completing the transition and reappears only above ~20 GPa. Upon decompression from high pressures, the scattering intensity remains rather high at least down to 1 GPa. The inset shows an approximation of the spectrum measured at 8.2 GPa.

1 Amiel, Y. et al. Silvanite AuAgTe4: a rare case of gold superconducting material, *J. Mater. Chem.* C **11**, 10016–10024 (2023).

2 Sterer, E., Pasternak, M. P. and Taylor, R. D., *Rev. Sci. Instrum.* **61**, 1117 (1990), URL https://doi.org/10.1063/1.1141433.

3 Kantor, I., Prakapenka V., Kantor, A., et al., *Rev. Sci. Instrum*. **83**, 125102 (2012)

4 Prescher, C., & Prakapenka, V. B., DIOPTAS: a program for reduction of two-dimensional X-ray diffraction data and data exploration. *High Pressure Research*, **35**(3), 223-230 (2015).

5 Toby, B. H., & Von Dreele, R. B., GSAS-II: the genesis of a modern open-source all purpose crystallography software package. *Applied Crystallography*, **46**(2), 544-549 (2013).

6 Rodríguez-Carvajal, J., Study of micro-structural effects by powder diffraction using the program FULLPROF. *Laboratoire Leon Brillouin* (CEA-CNRS) (2022).

7 Holtgrewe, N., Greenberg, E., Prescher, C., Prakapenka, V. B., & Goncharov, A. F., Advanced integrated optical spectroscopy system for diamond anvil cell studies at GSECARS. *High Pressure Research*, **39**(3), 457-470 (2019).